# Steady states for viscous fingers with anisotropic surface tension

Eugenia Corvera and Hong Guo
*Centre for the Physics of Materials, Department of Physics, McGill University, Montréal, Québec, Canada H3A 2T8*

David Jasnow
*Department of Physics and Astronomy, University of Pittsburgh, Pittsburgh, Pennsylvania 15260*
(Received 7 November 1994)

Pattern selection is considered for the case of viscous fingering in rectangular Hele-Shaw geometry in the presence of anisotropic surface tension, using solvability analysis and a boundary-integral method. We find that anisotropy introduced as a sinusoidal perturbation with a fourfold symmetry is irrelevant for small driving velocities and the usual steady-state finger width in the absence of the anisotropy is obtained. For sufficiently large driving velocities a new steady-state width is selected when the anisotropy makes the local interfacial tension a maximum at the finger tip. This is in agreement with recent experimental observations.

PACS number(s): 05.70.Ln, 68.35.Fx, 82.65.Dp

Selection in the Saffman-Taylor (ST) problem [1] involves the prediction of the steady-state shape of the fluid interface in a two-phase flow confined in an effectively two dimensional channel, a Hele-Shaw cell, where a less viscous fluid displaces a more viscous one. This problem is a prototype for a class of pattern-forming systems in which interfacial instabilities [2] evolve, lead to the growth of interfacial structures, and eventually to the selection of well-defined steady-state patterns. In this case a competition mechanism leads to a single finger-shaped pattern (the ST finger) in the Hele-Shaw cell at large times [3]. Experimentally [1, 4] the steady-state finger is characterized by its width $\lambda$ which is a unique function of a control parameter $\gamma \equiv \frac{\tau}{12\mu v_\infty}\left(\frac{b}{a}\right)^2$, where $\tau$ is the interfacial tension, $\mu$ is the viscosity of the displaced fluid, $b$ is the gap spacing of the Hele-Shaw cell, $2a = W$ is the channel width, and $v_\infty$ is the velocity of the fluid very far ahead of the interface. In standard Hele-Shaw experiments one finds $\lambda > \frac{1}{2}W$. The control parameter $\gamma$ provides a singular perturbation to the zero-surface-tension equations of motion describing the Hele-Shaw flow [5], and several experiments were carried out to alter this parameter and study the system response. New steady-state patterns were observed in these "perturbed" Hele-Shaw cells [6–9].

In this paper we report a theoretical study of Hele-Shaw flow when the surface tension is modified by the addition of an anisotropic contribution. It is known from experiments [10] and simulations of Sarkar and Jasnow [11] and Almgren *et al.* [12] that even a small anisotropy can produce drastic effects on the patterns for viscous fingering in *circular* rather than rectangular geometry. Experimentally, such a term can be introduced if one of the bounding plates is etched with small grooves with a regular spacing that is small compared to the size of the patterns [11, 13]. Recently a systematic experimental study of this situation has been carried out by McCloud and Maher [14]. Our theoretical results are found to be consistent with the measurements in the appropriate parameter range.

We have carried out a solvability analysis that includes anisotropic interfacial tension. Solutions were found in addition to the solutions for isotropic interfacial tension. The steady-state pattern selection was also studied using a boundary-integral method to numerically solve the governing equations. When the system is driven at a large enough velocity and anisotropy makes the local interfacial tension a *maximum* at the fingertip, the late time finger is distinctly wider than in the corresponding isotropic case. The numerical solutions are in qualitative agreement with the solvability analysis. The results taken together suggest a wider, steady state in the presence of anisotropic interfacial tension. This is significant in view of the prototypical role this system plays in the study of pattern selection and in view of the subtle effect of anisotropy.

We specialize to the case of high viscosity contrast. McLean and Saffman [15] used conformal methods to transform the equation of motion for the flow into an integro-differential equation. If the surface tension is allowed to be anisotropic, the original equation [15] is modified to give

$$qs\frac{d}{ds}\left[\nu_a qs\frac{d\theta}{ds}\right] = q - \cos\theta\ , \tag{1}$$

$$\ln_{10} q(s) = -\frac{s}{\pi}\,\mathrm{P}\int_0^1 ds'\frac{\theta(s')}{s'(s'-s)}, \tag{2}$$

$$\nu_a = \nu(1 - \epsilon f(\theta)). \tag{3}$$

Here $\nu = \gamma\pi^2\frac{\lambda}{(1-\lambda)^2}$. The parameter $\theta$ is the angle of orientation of the interface, and $s$ parametrizes the interface, running from $s = 1$ at the "tip" to $s = 0$ at the "tail"; $\theta(1) = -\pi/2$ and $\theta(0) = 0$. We assume that the anisotropy coefficient $\epsilon$ is small. The zero-surface-tension solution is, as in the isotropic case [15], $q_0(s) =$

 

$\cos\theta_0(s) = \left[\frac{1-s}{1+\alpha s}\right]^{\frac{1}{2}}$, where $\alpha = (2\lambda-1)/(1-\lambda)^2$. We study the effect of a fourfold symmetry for the anisotropy and choose $f(\theta) = \cos 4\theta$ [11]. Using the standard solvability analysis [8, 16], we linearize Eq. (1) around $\theta(s) = \theta_0(s) + \nu\theta_1(s)$ and carrying out a singular perturbation expansion. In particular, we neglect terms quadratic in $\epsilon$ and terms quadratic in $\nu$ and terms cubic in $\nu$ multiplying derivatives of $\theta_1$. Furthermore, since the anisotropic parameter $\epsilon$ is small, we neglect terms quadratic in $\epsilon$ and terms linear in $\epsilon$ and quadratic in $\nu$ multiplying derivatives of $\theta_1$. Our approximation is valid as long as $|\epsilon|$ is of the order $\nu$ or smaller. Next the variable $s$ is replaced by $\eta = \left[\frac{1-s}{(1+\alpha)s}\right]^{\frac{1}{2}}$, which in terms of Cartesian coordinates is the slope varying from $-\infty$ to $\infty$ passing through $\eta = 0$ at the tip of the finger. Finally the above equation is simplified after a further change of variable $\Theta(\eta) = \frac{(1+\beta^2\eta^2)^{1/2}}{(1+\eta^2)^{1/4}}\theta_1(\eta)$, where $\beta = (1+\alpha)^{1/2} = \lambda/(1-\lambda)$. This yields an equation of the form

$$\mathcal{L}\Theta(\eta) = R_A(\eta), \tag{4}$$

where the left-hand side [17] is the same as in the case of isotropic surface tension [8]. The right-hand side of (4) is given by $R_A(\eta) = R(\eta)(1-\epsilon\cos 4\theta_0) + R^*(\eta)$, where

$$R(\eta) = \frac{\eta[3+\beta^2(\eta^2-2)]}{(1+\beta^2\eta^2)^{\frac{1}{2}}(1+\eta^2)^{\frac{9}{4}}},$$

$$\cos 4\theta_0 = \frac{\eta^4 - 6\eta^2 + 1}{(\eta^2+1)^2},$$

and

$$R^*(\eta) = \epsilon\frac{16\eta(1+\beta^2\eta^2)^{1/2}(1-\eta^2)}{(\eta^2+1)^{17/4}}.$$

The next step of standard solvability analysis [8] is to consider the "cusp function"

$$\Lambda \equiv \int_{-\infty}^{\infty} d\eta\, \Theta_0 R_A(\eta), \tag{5}$$

where $\Theta_0$ satisfies $\mathcal{L}^\dagger\Theta_0 = 0$ and $\mathcal{L}^\dagger$ is the adjoint of the operator $\mathcal{L}$. Since the left-hand side of Eq. (4) is exactly the same as for the isotropic case, the solution of Hong and Langer for the null eigenvector $\Theta_0$ is still valid for our case. Using Ref. [8] the null eigenvector $\Theta_0$ is equal to the imaginary part of $\Theta_{0_+}$ given by $\Theta_{0_+} = e^{\frac{\Psi_+}{\sqrt{\nu}}}/Q_+^{1/4}$, where $\frac{d\Psi_+}{d\eta} = iQ_+^{1/2}$ and $Q_+(\eta) = \frac{4\beta^4(1+i\eta)^{\frac{3}{2}}(1-i\eta)^{\frac{1}{2}}}{(1+\beta^2\eta^2)^2}$. $\Lambda(\lambda,\nu,\epsilon)$ can be evaluated by the method of steepest descent.

Because of the analytical structure of the functions in Eq. (5), two distinct situations occur depending on the range of values of the finger width $\lambda$ [8]. For the case $\lambda < 1/2$ the normalized cusp function is [18]

$$\Lambda(\lambda,\nu,\epsilon) = e^{\frac{E(\lambda)}{\sqrt{\nu}}}\left\{a_1 g^{1/14} - a_2\frac{\epsilon}{g^{15/14}}\right\}. \tag{6}$$

For $\lambda > 1/2$, the integral in the exponential term of $\Theta_0$ has a pole inside the contour of integration, and the cusp function has an extra term. One finds

$$\Lambda(\lambda,\nu,\epsilon) = e^{\frac{E(\lambda)}{\sqrt{\nu}}}\left\{a_1(-g)^{1/14} + a_2\frac{\epsilon}{(-g)^{15/14}}\right\} \times \cos\frac{2\pi(2\lambda-1)^{\frac{3}{4}}}{\nu^{\frac{1}{2}}(1-\lambda)}. \tag{7}$$

In the above expressions

$$g = \left[\frac{(1-2\lambda)\nu^{1/2}}{\lambda^2}\right],$$

$$a_1 = 3\pi\frac{2^{23/14}}{7^{27/14}}\frac{1}{\Gamma(27/14)}, \quad a_2 = \pi\frac{2^{89/14}}{7^{29/14}}\frac{1}{\Gamma(43/14)}.$$

The zeros of the cusp function provide the solvability condition that leads to a relationship between $\lambda$, $\nu$, and $\epsilon$. For $\epsilon > 0$ the cusp function of Eq. (6) may vanish; thus a possible solution for $\lambda < 1/2$ exists. This has been found by Dorsey and Martin [19] using a numerical nonlinear eigenvalue method. Close to (but below) $\lambda = 1/2$, we find $\lambda \simeq \frac{1}{2} - \frac{1}{2^3}\left(\frac{a_2}{a_1}\right)^{7/8}\frac{(\epsilon)^{7/8}}{\nu^{\frac{1}{2}}}$; and close to $\lambda = 0$, $\lambda \simeq \left(\frac{a_1}{a_2}\right)^{7/16}\frac{(\nu)^{1/4}}{\epsilon^{\frac{7}{16}}}$. These asymptotic scalings, i.e., $\nu \sim \epsilon^{7/4}$ at fixed $\lambda \simeq 1/2$, and $\lambda \sim \nu^{1/4}$ for small $\lambda$ at fixed $\epsilon$, were obtained previously for dendritic growth in a channel in the limit in which it is mathematically equivalent to the Hele-Shaw problem [20]. For $\lambda > 1/2$, the cusp function (7) can vanish because of the cosine term, thus predicting that close to $\lambda = 1/2$ the finger width increases with $\nu$ as

$$\lambda \simeq \frac{1}{2} + \frac{1}{2^5}\nu^{\frac{2}{3}}. \tag{8}$$

This is exactly the same solution as that of the isotropic interfacial tension case. Thus for a positive $\epsilon$, namely when local interfacial tension has a *minimum* at the fingertip, there are two possible solutions: one for $\lambda < 1/2$; the other for $\lambda > 1/2$, with a width that is the same as that of the steady-state finger with isotropic surface tension. Our numerical results presented below indicate that it is the $\lambda > 1/2$ solution that is actually selected. When $\epsilon < 0$, i.e., when the local interfacial tension has a *maximum* value at the fingertip, the cusp function (6) cannot vanish; thus no solution for $\lambda < 1/2$ exists. On the other hand, for $\lambda > 1/2$ the zeros of the cusp function can be given by either of the two terms multiplying the exponential in (7) [22]. The vanishing of the cosine leads to Eq. (8). A new solution is given by the vanishing of the other multiplicative term in (7), and close to $\lambda = 1/2$ is

$$\lambda \simeq \frac{1}{2} + \frac{1}{2^3}\left(\frac{a_2}{a_1}\right)^{7/8}\frac{(-\epsilon)^{7/8}}{\nu^{\frac{1}{2}}}. \tag{9}$$

Since intuitively we expect that larger interfacial tension at the tip leads to a wider finger, the new solution may be physically viable if it does give a larger $\lambda$. This happens when $\nu$ is smaller than $\nu_c \equiv 2^{12/7}\left(\frac{a_2}{a_1}\right)^{3/4}(-\epsilon)^{3/4}$. Thus

for small $\nu$, or large driving velocity, a new steady state may be selected [21]. On the other hand, for $\nu > \nu_c$ or small driving velocity, Eq. (8) gives a wider finger, and the same steady state as that of the isotropic case should be recovered.

Whether or not a solution is selected by nature can only be answered by additional considerations. Here we decided to simulate the experimental situation by numerically solving the flow equations and following the dynamical evolution of the pattern as it develops from an initially near flat shape. The numerical method used is standard [23]. The equation to be integrated is of the form

$$\frac{C(s)}{2} - \int_0^{S_{tot}} ds' \hat{\mathbf{n}} \cdot \nabla' G(s,s') C(s') = \int_0^{S_{tot}} ds' G(s,s') v_n(s'), \quad (10)$$

where the interface shape is parametrized by the contour variable $s$. The integration extends over the entire contour of length $S_{tot}$ in a channel of width $W$. The Green's function $G(s,s') \equiv G(\mathbf{r}(s),\mathbf{r}(s'))$ satisfies $\nabla'^2 G(\mathbf{r},\mathbf{r}') = -\delta(\mathbf{r}-\mathbf{r}')$, with periodic boundary conditions in the direction transverse to the flow direction [23]. In (10), $v_n$ is the normal velocity of the interface. $C(s)$ is essentially the pressure at the interface $C(s) = d_0(1+\delta-\delta\cos 4\theta(s))\kappa(s) + \xi(s)/l$, where $\theta(s)$ is the angle of the normal to the interface (into the displaced fluid) with respect to the channel direction, $\kappa(s)$ is the local curvature, and the length $\xi$ measures the displacement from the (unstable) flat interface that would advance with $v_\infty \sim 1/l$. The parameter $d_0$ is a capillary length, and in terms of suitably dimensionless variables, the control parameter $\gamma$ introduced previously is given by $\gamma = 4d_0 l/W^2$. Finally $\delta$ is a measure of the anisotropy. For purposes of numerical comparisons it was judged advantageous to keep the surface tension at the tip fixed, even with the introduction of anisotropy. The relation to the anisotropy $\epsilon$ introduced in (3) is $\delta/(1+\delta) = \epsilon$. Since we will only be considering relatively small $\delta$, there is no essential difference. All parameters are dimensionless at this stage. *Positive* $\delta \sim \epsilon$ makes the channel direction the "easy" direction with the tip having locally a *minimal* surface tension. A symmetric configuration $\xi(s)$ slightly perturbing a flat interface is given at the initial time. Then (10) is an integral equation for the normal velocities, $v_n(s)$. The position of the curve is updated and the process repeated. Further details are provided in Refs. [23, 24].

Simulations with a variety of parameter choices were run. Consistently it has been found that in the transient regime finger shapes are systematically narrower for $\delta > 0$ than for the isotropic case where $\delta = 0$, and they are systematically wider for $\delta < 0$. But then, as the finger develops, for relatively small driving velocity, the finger widths become indistinguishable from the isotropic case. This is true for values of $|\delta|$ up to 0.20, which is considerably larger than the anisotropy required to make a profound change on patterns in circular geometry [11]. Qualitatively this is reasonable since the sidewalls already introduce effective anisotropy, which for small driving velocity may overwhelm a small additional local anisotropy.

Several representative runs are now shown. The first examples have $d_0 = 1.0$, $1/l = v_\infty = 0.01$, and $W = 60$, corresponding to $\gamma \sim 0.1$. Parameters were chosen here to yield a value of $\lambda$ significantly larger than one-half. In Fig. 1 the early time behavior for the isotropic case ($\delta = 0$) and $\delta = \pm 0.10$ are shown. The initial condition is the same for all cases. Although the patterns shown are not very well defined fingers at this early time, the widths are becoming roughly the same while, early on, the shapes are observably different. At intermediate times ($t = 25 - 50 \times 10^3$) the fingers become better defined, with essentially equal widths. In Fig. 2 the final fingertip regions are shown superimposed by making the tip positions agree. The three cases are virtually indistinguishable. To the precision of the simulations the shape of the tip is at most weakly dependent on the anisotropy. Note that in the final time shown in Fig. 2 the total extent of the structure is about 1000 in the channel direction, but down at the tail there are still oscillations that damp out as one moves toward the tip. Our numerical results on the dynamical growth indicate that a wider finger can be generated for negative $\delta \sim \epsilon$ at sufficiently small $\gamma$. In Fig. 3 an example run is shown with the effective driving force $\gamma$ increased by a factor of 30. The relative anisotropy remains at $\epsilon \simeq \delta = -0.1$, which again makes the surface tension at the tip a local maximum. Reversing the sign of $\delta$ did not appear to produce a finger narrower than the isotropic one. This seems to suggest that the solution for $\lambda < 1/2$ found by our solvability analysis as well as in Refs. [19, 20] is not actually selected, at least within the range of parameters of the simulations. This would imply that the small anisotropy introduced by $\delta > 0$, which would make the channel direction "easier" for the finger to advance, is negligible compared to the effect of the sidewalls that al-

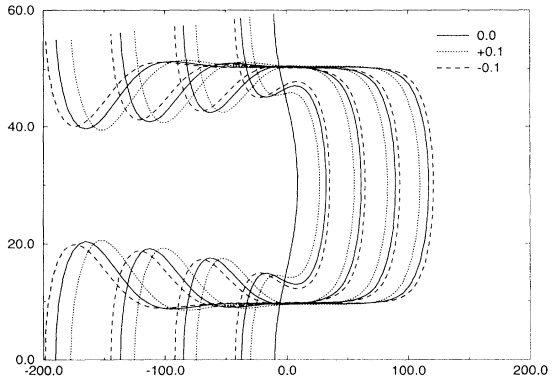


FIG. 1. Early time evolution of the finger structure. The solid line near the center is the initial condition in all cases. The legend indicates the value of surface tension anisotropy $\delta$. The different sets of curves indicate dimensionless times equally spaced from zero to $t = 25\,000$.

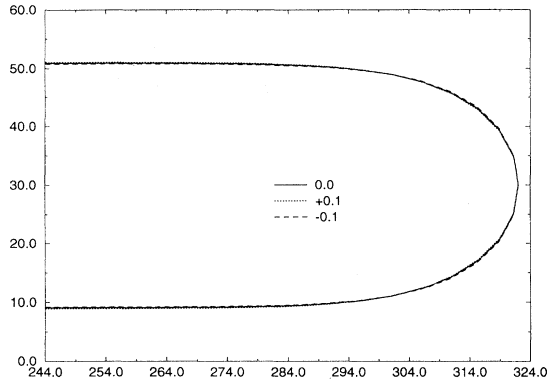


FIG. 2. Tip region at $t = 75\,000$. Notice that the entire finger structure covers a length of about 1000 along the channel direction. The two anisotropic curves are rigidly translated in the channel direction so that tip positions agree with that of the curve for isotropic surface tension.

ready provide an effective anisotropy, which makes the channel direction "the easy" direction. Our numerical limits were reached before the anisotropic finger clearly settled down after a transient period of widening out to the corresponding isotropic finger. Numerical difficulties prevented us from using larger driving forces in the simulation, so that the selection of a narrower finger at very small $\nu$ and $\epsilon$ cannot be ruled out. For the case of $\delta < 0$, the anisotropy introduced does not favor the same direction, which is naturally favored by the walls, and its effect gives rise to a different solution.

The *dynamical evolution* of the pattern, at early to intermediate times, is clearly dependent on the interfacial tension anisotropy strength $\epsilon$. However, our numerical results, taken together with the solvability analysis, indicate that, for a sufficiently low driving force, anisotropy in the local interfacial tension in the form of Eq. (3) is irrelevant for steady-state finger widths in a rectangular Hele-Shaw cell with high viscosity contrast. On the other hand, when anisotropy makes the local interfacial tension a maximum at the fingertip, and when the driving velocity is sufficiently large, both theory and numerical simulation predict a solution that gives a wider finger than the corresponding solution with isotropic interfacial tension. Due to the narrow range of $\nu$ in which the solvability analysis is valid [21], it is only possible for us to compare qualitatively the theory with numerical simulations. Indeed, both methods predict a new steady state that should be observable in an experimental setup that can cleanly control the fourfold surface tension anisotropy. We are therefore suggesting a new steady-state pattern in the presence of anisotropy. We conjecture that for $\epsilon < 0$ the system will choose from the two plausible solutions the one that predicts the wider finger. This conjecture puts the analytical results of the solvability analysis and the dynamical simulations into a consistent picture.

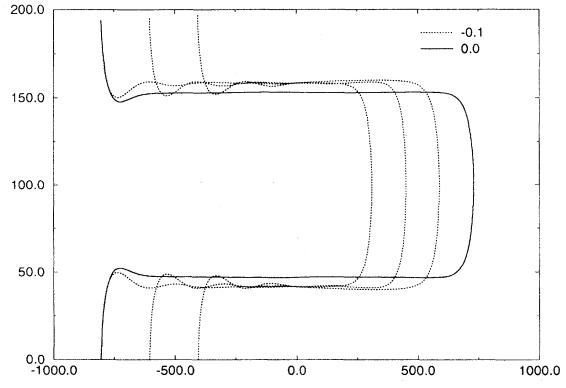


FIG. 3. Finger evolution for larger driving force $\gamma = 4d_0/v_\infty W^2 \sim 0.004$, with $\delta = -0.1$ suggesting a wider finger than the corresponding isotropic one (solid line).

This physical picture is also consistent with the very recent experiments of McCloud and Maher [14], where they have etched the bounding plates of the Hele-Shaw cell to produce an effective anisotropy. In particular, our theoretical results presented above give a qualitative explanation of their experiments when the perturbation due to anisotropy can be considered as microscopic [14]. In McCloud and Maher's experiments, for system parameters that produce a large $\nu$, such as a wide cell gap or small driving velocity, the etched lattices have no observable effect on the ST finger, i.e., the finger is the same as that of the unperturbed flow, and the lattice anisotropy is essentially irrelevant. On the other hand, for small $\nu$, a wider finger is systematically observed, and the change from the usual ST finger to the wider one is apparently sharp as the parameter $\nu$ is reduced. Experimentally the anisotropy can be varied using different cell gaps [14], and the selection of the wider fingers does not set in abruptly at some very large value of anisotropy. It appears smoothly as the anisotropy is increased, with small anisotropies yielding results indistinguishable from the ST values and larger anisotropies showing stronger effects. Our theoretical results presented above are consistent with these observations. Comparisons with our theoretical results have been partially made in McCloud and Maher's article [14]; we refer interested readers to that reference for more details.

Finally, we note that experiments that produce markedly changed steady states, such as those in Refs. [6, 7], may actually introduce nonlocal effects or other effects not included in the simplest modeling done here. Furthermore, we have not treated *kinetic* anisotropy, which would be included in the boundary condition at the interface as a term of the form $\beta(\theta)v_n$, where the coefficient $\beta$ has fourfold symmetry [11]. Preliminary simulations indicate that kinetic anisotropy can control the finger width and may play a role in the experiments. It will be interesting to consider these effects in a further analysis.

E.C. and H.G. thank Jianhua Yao and Daniel Hong for useful discussions. E.C. thanks Kathy McCloud for useful discussions of her unpublished experimental work. H.G. is supported in part by NSERC, and by FCAR. E.C. is supported by CIDA and CONACYT. D.J. gratefully acknowledges support of the NSF, under Grant No. DMR92-17935, and thanks the Pittsburgh Supercomputing Center.

[1] P. G. Saffman and G. I. Taylor, Proc. R. Soc. London Ser. A **245**, 312 (1958); P. G. Saffman, J. Fluid Mech. **173**, 73 (1986).
[2] W. W. Mullins and R. F. Sekerka, J. Appl. Phys. **34**, 323 (1963).
[3] D. Jasnow and J. Viñals, Phys. Rev. A **41**, 6910 (1990); H. Guo, D. C. Hong, and D. A. Kurtze, *ibid.* **46**, 1867 (1992).
[4] P. Tabeling and A. Libchaber, Phys. Rev. A **33**, 794 (1986); P. Tabeling, G. Zocchi, and A. Libchaber, J. Fluid Mech. **177**, 67 (1987).
[5] B. Schraiman, Phys. Rev. Lett. **56**, 2028 (1986); D. C. Hong and J. S. Langer, *ibid.* 2032 (1986); R. Combescot, T. Dombre, V. Hakim, Y. Pomeau, and A. Pumir, *ibid.* 2036 (1986).
[6] Y. Couder, N. Gérard, and M. Rabaud, Phys. Rev. A **34**, 5175 (1986); Y. Couder, O. Cardoso, D. Dupuy, P. Tavernier, and W. Thom, Europhys. Lett. **2**, 437 (1986).
[7] G. Zocchi, B. Shaw, A. Libchaber, and L. Kadanoff, Phys. Rev. A **36**, 1894 (1987).
[8] D. C. Hong and J. S. Langer, Phys. Rev. A **36**, 2325 (1987).
[9] H. Guo and D.C. Hong, Phys. Rev. A **41**, 2995 (1990).
[10] E. Ben-Jacob, R. Godbey, Nigel D. Goldenfeld, J. Koplik, H. Levine, T. Mueller, and L.M. Sander, Phys. Rev. Lett. **55**, 1315 (1985).
[11] S. K. Sarkar and D. Jasnow, Phys. Rev. A **39**, 5299 (1989).
[12] R. Almgren, W.-S. Dai, and V. Hakim, Phys. Rev. Lett. **71**, 3461 (1993).
[13] J. D. Chen, Exp. Fluids **5**, 363 (1987).
[14] K. McCloud and J. Maher, Phys. Rev. E **51**, 1184 (1995).
[15] J. W. McLean and P. G. Saffman, J. Fluid Mech. **102**, 455 (1981).
[16] J. S. Langer, in *Le hasard et la matière Chance and Matter*, Les Houches, Session XLVI, 1986, edited by J. Souletie, J. Vannimenus, and R. Stora (North-Holland, Amsterdam, 1987); D. Kessler, J. Koplik, and H. Levine, Adv. Phys. **37**, 255 (1988).
[17] The explicit form of the left-hand side of Eq. (4) is not necessary to follow the remainder of the paper. It can be founded explicitly in Ref. [8].
[18] E. Corvera, Phys. Rev. E **48**, 964 (1993).
[19] A. T. Dorsey and O. Martin, Phys. Rev. A **35**, 3989 (1987).
[20] D. A. Kessler, J. Koplik, and H. Levine, Phys. Rev. A **34**, 4980 (1986).
[21] Since our approximation in the solvability analysis requires $-\epsilon < \nu$, the result of this analysis is valid when this condition is satisfied.
[22] M. Ben Amar, R. Combescot, and Y. Couder, Phys. Rev. Lett. **70**, 3047 (1993); R. Combescot, Phys. Rev. E **49**, 4172 (1994).
[23] J. Viñals and D. Jasnow, Phys. Rev. A **46**, 7777 (1992).
[24] J. Viñals and D. Jasnow, in *Computer Simulations in Condensed Matter Physics IV*, edited by D. P. Landau, K. K. Mon, and H. B. Shuttler (Springer-Verlag, New York, 1992).